A Kinetic and Stereochemical Investigation of the Role of Lysine-32 in the Phenylpyruvate Tautomerase Activity Catalyzed by Macrophage Migration Inhibitory Factor†

William H. Johnson, Jr., Robert M. Czerwinski, Stacy L. Stamps, and Christian P. Whitman*

Medicinal Chemistry Division, College of Pharmacy, The University of Texas, Austin, Texas 78712-1074

Received August 5, 1999; Revised Manuscript Received September 28, 1999

ABSTRACT: Macrophage migration inhibitory factor (MIF), an immunoregulatory protein, exhibits a phenylpyruvate tautomerase (PPT) activity. The catalytic mechanism of this activity has recently attracted attention in an effort to determine whether there is a relationship between the PPT activity and the role of MIF in various immune and inflammatory processes. One of the active site residues is lysine-32, which is postulated to play two roles: it assists in substrate binding through an interaction with a carboxylate oxygen at C-1 of phenylpyruvate, and it may be partially responsible for lowering the pK_a of the catalytic base, Pro-1. The role of Lys-32 has been investigated by changing it to an alanine and an arginine and determining the kinetic parameters, the stereoselectivity, the competitive inhibition, and the pH dependence of the resulting K32A- and K32R-catalyzed reactions. For the K32R mutant, these properties are mostly comparable to those determined for the wild type with two exceptions. There is a modest decrease in the stereoselectivity of the reaction and in the binding affinity of the competitive inhibitor, (*E*)-2-fluoro-*p*-hydroxycinnamate. These differences are likely due to the increased steric bulk of arginine. For the K32A mutant, there are 11- and 12-fold decreases in k_{cat} and k_{cat}/K_m, respectively, using phenylenolpyruvate. Part of the decrease in activity can be attributed to the observed increase of 1.3 units in the pK_a of Pro-1. It was also found that the loss of the electrostatic interaction did not significantly affect the stereoselectivity of the K32A-catalyzed reaction, although it did result in a decrease in the binding affinity of the competitive inhibitor. The combination of these results indicates that the primary function of Lys-32 in the PPT activity of MIF is to lower the pK_a of Pro-1. The interactions responsible for the stereoselectivity of the PPT activity were further delineated by examining the wild type- and K32A-catalyzed reactions with an alternate substrate, 2-hydroxy-2,4-pentadienoate, in which the phenyl group of phenylenolpyruvate is replaced with a double bond. The effect of this substitution is moderate as evidenced by the observation that the ketonization of 2-hydroxy-2,4-pentadienoate by the wild type protein is more stereoselective than the K32R-catalyzed ketonization of phenylenolpyruvate but not as stereoselective as the K32A-catalyzed ketonization of phenylenolpyruvate. However, the low degree of stereoselectivity observed for the K32A-catalyzed reaction indicates that an electrostatic interaction between the protein and 2-hydroxy-2,4-pentadienoate is now crucial.

Macrophage migration inhibitory factor (MIF)[1] was among the first cytokine activities identified and has since been implicated in a variety of immune and inflammatory processes (*1*−*4*). Because MIF plays a role in sepsis (*5*), and may be involved in the pathogenesis of adult respiratory distress syndrome (*6*), rheumatoid arthritis (*7*), and glomerulonephritis (*7*), it is a potential therapeutic target. One possible avenue for the design of such therapeutics makes use of the observation that MIF exhibits an enzymatic activity (*8*). It catalyzes the enolization of dopachrome (**1**) to generate **2** (Scheme 1), and it interconverts the enol and keto isomers of both phenylpyruvate (**3** → **4**, Scheme 2) and (*p*-hydroxyphenyl)pyruvate (**5** → **6**, Scheme 2). The latter enzymatic activity coupled with other experimental evidence

Scheme 1

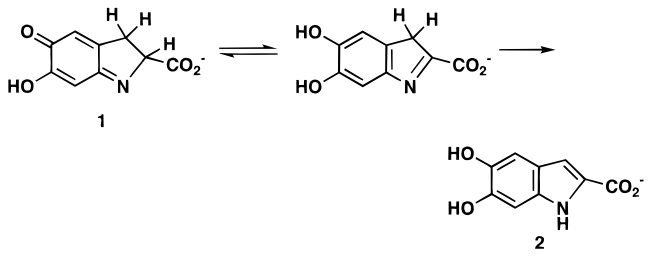

† This research was supported by the Texas Advanced Research Program (ARP-183).

* To whom correspondence should be addressed. Telephone: (512) 471-6198. Fax: (512) 232-2606. E-mail: cwhitman@uts.cc.utexas.edu.

[1] Abbreviations: BCA, bicinchoninic acid; CHMI, 5-(carboxymethyl)-2-hydroxymuconate isomerase; DEAE, diethylaminoethyl; DMSO-d_6, perdeuterated dimethyl sulfoxide; ESI-MS, electrospray ionization mass spectrometry; HPLC, high-pressure liquid chromatography; IPTG, isopropyl β-D-thiogalactoside; Kn, kanamycin; LB, Luria-Bertani medium; MIF, macrophage migration inhibitory factor; NMR, nuclear magnetic resonance; 4-OT, 4-oxalocrotonate tautomerase; PPT, phenylpyruvate tautomerase; PCR, polymerase chain reaction; SDS−PAGE, sodium dodecyl sulfate−polyacrylamide gel electrophoresis.

10.1021/bi991825s CCC: $18.00
Published on Web 11/09/1999

Scheme 2

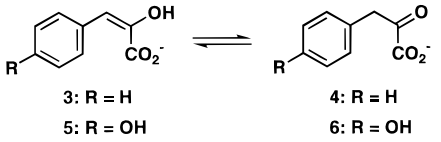

3: R = H **4**: R = H

5: R = OH **6**: R = OH

Scheme 3

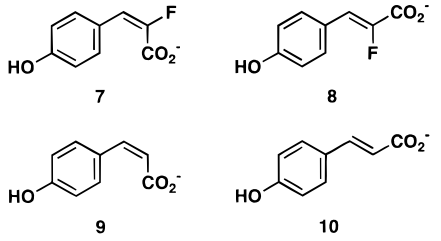

7 **8**

9 **10**

led to the conclusion that MIF and phenylpyruvate tautomerase (PPT) are the same protein (*8*).

Although it remains uncertain whether there is a connection between the PPT activity of MIF and its other biological activities, the elucidation of the catalytic mechanism of the PPT activity would certainly be useful if a link between these activities were established (*9*, *10*). Hence, the mechanism and the active site structure of MIF's PPT activity have come under scrutiny recently (*9*−*13*). On the basis of these studies, Pro-1 has been implicated as the catalytic base with a pK_a value of ∼6.0 (*10*, *11*).

In addition to Pro-1, two recent crystal structures identified Lys-32, Ile-64, Tyr-95, and Asn-97 as active site residues and suggested that Lys-32 plays a prominent role in the binding of the substrate's carboxylate group (*12*, *13*). In a crystal structure of MIF complexed with the competitive inhibitor (*E*)-2-fluoro-*p*-hydroxycinnamate (**7**, Scheme 3), one carboxylate oxygen is within 2.9 Å of the ammonium group of Lys-32 while the other carboxylate oxygen is within 2.4 Å of the nitrogen of Pro-1 (*12*). In a crystal structure of the MIF•**5** complex, one carboxylate oxygen is within 2.6 Å of the ammonium group of Lys-32 and the other carboxylate oxygen is within 2.7 Å of the backbone amide of Ile-64 (*13*). These crystallographic observations are consistent with the differential inhibition data reported for a series of enol analogue inhibitors of PPT (**7**−**10**, Scheme 3) (*14*). It was found that the (*E*)-**7** is a more potent inhibitor than its isomeric counterpart, (*Z*)-**8**, and (*Z*)-**9** is a more potent inhibitor than its isomeric counterpart, (*E*)-**10** (*14*). The differences in potencies are presumably due in part to the interaction between the carboxylate group and Lys-32 (*12*). It is interesting to note that Pro-1 and Lys-32 (along with Ile-64) are among the few invariant residues in all known MIF homologues (*10*, *13*).

Lys-32 may play another role in the PPT activity. The unusually low pK_a value of Pro-1 has been attributed to its location within a hydrophobic environment coupled with its proximity to two cationic residues, Lys-66 and Lys-32 (*10*, *13*). Support for this hypothesis comes from studies of a mutant of MIF in which an alanine is inserted between Pro-1 and Met-2. Titration of Pro-1 indicated that the pK_a value is further reduced (*13*). A crystal structure of the mutant demonstrated that Pro-1 was now "pushed out" of the hydrophobic cavity and positioned closer to Lys-32 and Lys-66.

To elucidate the contribution made by Lys-32 to the PPT activity, two mutants of MIF were constructed in which Lys-32 was replaced with either an alanine or an arginine. Subsequently, the kinetic parameters, the pH−rate profiles, the competitive inhibition by **7** and **10**, and the stereoselectivity of each mutant-catalyzed reaction were determined and compared to those of the wild type. The results show that the interaction of Lys-32 with substrate is not a critical factor either in substrate binding or as a determinant of the stereoselectivity of the reaction. However, Lys-32 does contribute to the potency of **7** as a competitive inhibitor but not to that of **10**. More significant, though, is the observation that the proximity of Lys-32 or a similar cationic group such as arginine plays an important role in lowering the pK_a of the catalytic proline. Additional insight into the PPT activity of MIF was obtained by identifying the factors responsible for the stereoselectivity of the reaction. An examination of the wild type- and K32A-catalyzed ketonization of 2-hydroxy-2,4-pentadienoate to 2-oxo[3-D]-4-pentenoate in D_2O shows that replacing the phenyl group with a double bond results in a moderate decrease in the stereoselectivity of the reaction. Coupling this substitution with the loss of the electrostatic interaction between Lys-32 and the carboxylate group of substrate causes a major decrease in the stereoselectivity of the reaction. Collectively, these studies show why Lys-32 is important to the PPT activity of MIF and shed light on the factors governing the stereochemical fidelity of the reaction.

MATERIALS AND METHODS

Materials. All biochemicals were purchased from Sigma Chemical Co. Centricon (10 000 molecular weight cutoff) centrifugal microconcentrators and ultrafiltration membranes were purchased from Amicon. The clone containing recombinant mouse MIF was obtained from R. Bucala (The Picower Institute for Medical Research, Manhasset, NY). Reagents for the PCR were obtained from either Promega Corp. (Madison, WI) or Perkin-Elmer (Norwalk, CT). Restriction enzymes and other molecular biology reagents were obtained from Promega Corp. with the exception of the Geneclean II kit, which was purchased from Bio 101, Inc. (La Jolla, CA). Oligonucleotides for site-directed mutagenesis and DNA sequencing were synthesized by Oligos Etc. Inc. (Wilsonville, OR). The composition of the LB medium is described elsewhere (*15*). The syntheses of (*E*)-2-fluoro-*p*-hydroxycinnamic acid (**7**) and 2-hydroxy-2,4-pentadienoate (**14**) are described elsewhere (*14*, *16*).

General Methods. HPLC was performed on a Waters system using a Waters Protein Pak (DEAE-5PW) anion-exchange column. Protein concentrations were determined using the commercially available bicinchoninic acid (BCA) protein assay kit (Pierce Chemical Co., Rockford, IL). Protein was analyzed by sodium dodecyl sulfate−polyacrylamide gel electrophoresis (SDS−PAGE) under denaturing conditions on 12.5% gels (*17*). Kinetic data were obtained on a Hewlett-Packard 8452A diode array spectrophotometer. The cuvettes were mixed with a stir/add cuvette mixer. The kinetic data were fitted by nonlinear regression data analysis using the Grafit program (Erithacus Software Ltd., Staines, U.K.) obtained from Sigma Chemical Co. DNA sequencing was carried out at The University of Texas Sequencing Facility. NMR spectra were obtained on either a Bruker AM-250

spectrometer or a Varian Unity INOVA-500 spectrometer as noted in the text. Chemical shifts were referenced as noted below.

Site-Directed Mutagenesis. The two mutants of MIF were prepared using the gene for mouse MIF cloned into a pET-11b vector as the template (*2*). A *Nde*I restriction site and a *Bam*HI restriction site flank the gene. The K32A and K32R mutant proteins were constructed using the overlap extension polymerase chain reaction as described elsewhere (*18*). The external PCR primers were oligonucleotides 5′-GCGGATAA-CAATTCCCCTCT-3′ (designated primer A) and 5′-CT-CAGCTTCCTTTCGGGCTT-3′ (designated primer D). Primer A corresponds to the coding sequence of a region of the pET-11b vector ∼50 bp upstream from the *Nde*I restriction site, while primer D corresponds to the complementary sequence of the pET-11b vector ∼20 bp downstream from the *Bam*HI restriction site. For the K32A mutant, the internal primers were oligonucleotides 5′-GCCACCGGCGCGCCCGCACAG-3′ (designated primer C) and 5′-CTGTGCGGGCGCGCCG-GTGGC-3′ (designated primer B). For the K32R mutant, the internal primers were oligonucleotides 5′-GCCACCGGC-CGGCCCGCACA-3′ (designated primer C) and 5′-TGT-GCGGGCCGGCCGGTGGC-3′ (designated primer B). In each set of primers, primer C contains the codon for the desired mutation (underlined), while the remaining bases correspond to the coding sequence of the MIF gene. Primer B is the complementary primer with the desired codon underlined.

PCRs were carried out in a Perkin-Elmer DNA Thermocycler 480 using template DNA, synthetic primers, and the PCR reagents as described previously (*19*). In two separate PCRs, the AB and CD fragments were generated using the plasmid pET-11b as the template with primers A and B in one reaction and primers C and D in a second reaction as described previously (*19*). Subsequently, the mutated DNA fragment was produced by performing PCR on a mixture of the AB and CD fragments (5 μL each) using primers A and D. The mutated DNA fragment and the pET-24a (+) vector were digested with *Nde*I and *Bam*HI restriction enzymes, purified, and ligated using T4 DNA ligase following a previously described protocol (*19*). Aliquots of the resulting mixture were transformed into competent *Escherichia coli* JM109 cells as described elsewhere (*19*) and grown on LB/Kn (100 μg/mL) plates at 37 °C. Single colonies were chosen at random and grown in liquid LB/Kn medium (50−100 μg/mL). The newly constructed plasmid was isolated and sequenced to verify the mutation. Subsequently, the mutated plasmid was transformed as described above into *E. coli* strain BL21(DE3)pLysS for protein expression.

Overexpression and Purification of Recombinant MIF and the K32 Mutants. The recombinant enzymes were overexpressed using a previously described procedure (*12*). MIF and the K32 mutants were purified (>95% as judged by SDS−PAGE) by a published procedure (*12*). Activity was monitored by following the ketonization of **3** (*12*). The most active fractions were pooled and concentrated. Typically, the yield of purified enzyme per liter is ∼75 mg of MIF, ∼100 mg of K32R, and ∼35 mg of K32A.

Enzymatic Activity Assays. Two assays were used to measure the enzymatic activity of MIF as indicated in the text. In one assay, the enolization of **4** was followed using a previously described assay in which the enzyme-generated enol isomers form a complex with boric acid (*14*, *20*). Alternatively, enzyme activity was measured by following the rate of ketonization of **3** or **5** (*12*). The ketonization of **3** is monitored at 288 nm (ϵ = 17 300 M^{-1} cm^{-1}), and the ketonization of **5** is monitored at 300 nm (ϵ = 21 600 M^{-1} cm^{-1}). The assay mixture contains 50 mM Na_2HPO_4 buffer (1 mL, pH 6.5) and an aliquot of a solution of MIF sufficiently dilute (0.5−1.0 μL of a 2.3 mg/mL solution, final concentration of 93−186 nM) to yield an initial linear rate. The assay was initiated by the addition of a small quantity (1−3.3 μL) of either **3** or **5** from various stock solutions (5, 10, 20, or 50 mM) made up in ethanol. The crystalline **3** and **5** exist exclusively as the enol isomers (*21*). The concentration of substrate used to assay the enzymatic activity of MIF ranged from 10 to 150 μM. No significant inhibition of the enzymatic activity by ethanol is observed at concentrations of ≤0.5% (v/v).

Mass Spectrometry of MIF and the K32 Mutants. The masses of the purified wild type MIF and the purified mutant proteins were determined by electrospray ionization mass spectrometry (ESI-MS) using a LCG Finnigan octapole electrospray mass spectrometer. Samples for ESI-MS were prepared and analyzed as previously described (*22*). Typically, each protein elutes as a single peak ∼45 min after the injection. The observed monomeric molecular masses (MH^+) for MIF, K32A, and K32R were 12 371 (calcd 12 373 Da), 12 316 (calcd 12 316 Da), and 12 401 Da (calcd 12 401 Da), respectively.

Circular Dichroism Spectroscopy. Circular dichroism spectra of MIF, K32A, and K32R were measured in 50 mM sodium phosphate buffer (pH 6.5) at a concentration of approximately 10 μM using a 300 μL CD cell with an optical path length of 0.1 mm. CD spectra were recorded on a Jasco J-600 spectropolarimeter.

pH−Rate Profiles of MIF, K32A MIF, and K32R MIF. The pH dependence of the K32A- and K32R-catalyzed ketonization of **3** to **4** was determined at 24 °C using a previously described protocol with the following modifications (*19*). For the K32A mutant, the dependence was determined over the pH range of 4.9−8.4 and the final concentration of the enzyme was 1.6 (pH 4.9−6.1), 0.8 (pH 6.6−7.5), or 0.5 μM (pH 8.0−8.4). For the K32R mutant, the dependence was determined over the pH range of 4.8−8.4 and the final concentration of the enzyme was 1.5 (pH 4.8−5.5) or 0.7 μM (pH 6.1−8.4). It was necessary to use different enzyme concentrations to facilitate the measurement of the reduced rates at the extreme pH values. The reaction was initiated by the addition of a quantity of **3** from various stock solutions (5, 10, 20, or 50 mM) made up in ethanol. The final concentration of **3** ranged from 10 to 150 μM. The mutants were allowed to incubate in the assay buffer for 10 min before the addition of **3**. The reported pH is measured at the end of each assay. The initial rates were determined from plots of absorbance versus time at 288 nm and the data fitted as described previously (*19*).

Inhibition Studies with MIF, K32A, and K32R. The reversible competitive inhibition of MIF, K32A, and K32R by **10** was examined by following the enolization of **4** (*14*, *20*). Accordingly, the extent of inhibition was measured at increasing concentrations of **10** (0, 50, 75, 100, and 200 μM) in the presence of 11 concentrations of **4** (0.25−6.0 mM). A stock solution of **10** (50 mM) was made in 50 mM sodium

acetate buffer (final pH 7.0). The amount of enzyme used varied as follows: MIF, 5−15 μL of a 2.6 mg/mL solution; K32A, 5−15 μL of a 2.8 mg/mL solution; and K32R, 5−15 μL of a 3.9 mg/mL solution. Since **10** has a strong UV absorbance at 300 nm, the wavelength at which the rate of borate complex formation is usually followed (*14*, *20*), it was necessary to determine the initial rates from plots of absorbance versus time at 320 nm (ϵ = 4300 M^{-1} cm^{-1}) where the UV absorbance of **10** is less significant. The extent of reversible competitive inhibition of MIF, K32A, and K32R by **7** was determined by following the ketonization of **3** (*12*). Various concentrations of **7** (MIF, 0, 1, 2.5, 5, and 10 μM; K32A, 0, 10, 25, 50, and 100 μM; and K32R, 0, 1, 2.5, 5, 10, and 25 μM) were examined in the presence of 12 concentrations of **3** (10−150 μM). A stock solution of **7** (10 mM) was made up in 50 mM phosphate buffer (final pH 6.5). The amount of enzyme used varied as follows: MIF, 1 μL of a 1.1 mg/mL solution; K32A, 5 μL of a 2.0 mg/mL solution; and K32R, 1 μL of a 1.8 mg/mL solution. The initial rates were determined from plots of absorbance versus time at 288 nm. The kinetic data were fitted by nonlinear regression data analysis using the equation for competitive inhibition provided with the Grafit program.

*MIF-, K32A-, and K32R-Catalyzed Ketonization of **3** to [3-D]**4** in D_2O and Conversion of [3-D]**4** to [3-D]**11***. A solution of **3** (4 mg, 24 μmol) dissolved in DMSO-d_6 (30 μL) was added to 100 mM Na_2DPO_4 (0.6 mL, pD 9.3) buffer made up in D_2O. The addition of **3** (as the free acid) lowered the pD of the buffer to ~6.8. Enzyme (MIF, 30 μg; K32A, 120 μg; and K32R, 80 μg) was added to the reaction mixture immediately. Fifteen individual reaction mixtures were prepared for each enzyme. After 2.5 min, an aliquot of $NaBH_4$ (9 mg in 30 μL of 100 mM Na_2DPO_4 buffer) was added and the individual mixtures were allowed to stand overnight at room temperature. The reaction mixtures for each enzyme were pooled, and the pH was adjusted to 6.5 (using 8.5% phosphoric acid) to destroy the excess $NaBH_4$. After the bubbling had stopped, the pH was adjusted to 8 (using 5 M NaOH) and the solution was extracted with ethyl acetate (3 × 50 mL). Subsequently, the pH was adjusted to 1.5, and the solution was extracted with ethyl acetate (3 × 50 mL). The ethyl acetate layers (containing [3-D]**11**) were pooled, dried over anhydrous Na_2SO_4, filtered, and evaporated to dryness. To remove the residual DMSO-d_6, the resulting oil was heated at 55 °C under vacuum (1.5 mm) for 1.5 h to yield 60 (MIF and K32A) and 50 mg (K32R) of [3-D]**11**. The ^1H and ^{13}C NMR spectra corresponded to the previously reported spectra taking into account the deuterium substitution (*23*).

*Chemical and Enzymatic Conversion of [3-D]**11** to [3-D]-Malate (**13**).* To convert [3-D]**11** to [3-D]-D,L-malate (**12**), a solution of [3-D]**11** in 90% (v/v) acetic acid was subjected to a stream of O_3 at room temperature for 4.5 h (*24*). Subsequently, the mixture was purged with O_2, and a 30% solution of hydrogen peroxide (2 mL) was added. The solution was then stirred at room temperature for 2 days and concentrated by rotary evaporation. The concentrate was dissolved in 20 mM sodium phosphate buffer, and the pH of the solution was adjusted to 7.3. A total of 40 μL of catalase (4 mg/mL) was added in 5 μL portions over a 10−15 min period. After the bubbling had stopped, the pH was adjusted to 8, and the diastereomeric [3-D]-D,L-malate (**12**) was purified by anion-exchange chromatography as described to yield 18 mg of MIF, 20 mg of K32A, and 11 mg of K32R (*22*). The (2*S*)-isomer of [3-D]malate was removed by treating a solution of diastereomeric [3-D]-D,L-malate with malic enzyme as described previously (*22*, *25*). The (2*R*)-isomer was purified by anion-exchange chromatography as described previously (*22*) to afford 4.5 mg of MIF, 6.3 mg of K32A, and 2.2 mg of K32R. (2*R*,3*S*)-[3-D]Malate (**13**) (from the MIF-catalyzed reaction): ^1H NMR (CD_3OD, 500 MHz) δ 2.61 (1H, brd d, $J_{2,3}$ = 9.1 Hz, H3), 4.46 (1H, brd d, $J_{2,3}$ = 9.1 Hz, H2). (2*R*,3*S*)-[3-D]Malate (**13**) (from the K32A- and K32R-catalyzed reactions): ^1H NMR (CD_3OD, 500 MHz) δ 2.61 (K32A, 0.95H; K32R, 0.8H, brd d, $J_{2,3}$ = 9.0 Hz, H3), 4.46 (K32A, 0.95H; K32R, 0.8H, brd d, $J_{2,3}$ = 9.0 Hz, H2). (2*R*,3*R*)-[3-D]Malate (from the K32A- and K32R-catalyzed reactions): ^1H NMR (CD_3OD, 500 MHz) δ 2.76 (K32A, 0.05H; K32R, 0.2H, brd d, $J_{2,3}$ = 4.5 Hz, H3), 4.44 (K32A, 0.05H; K32R, 0.2H, brd s, H2).

Scheme 4

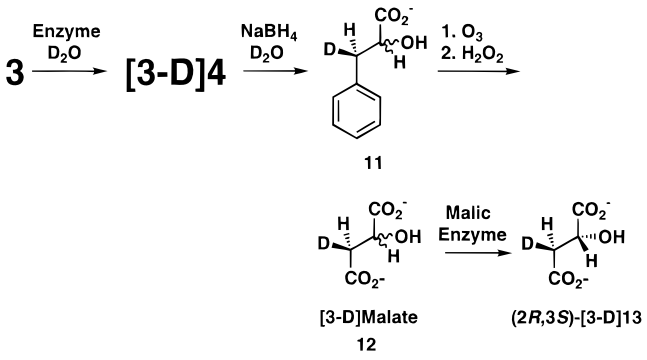

*MIF- and K32A-Catalyzed Ketonization of 2-Hydroxy-2,4-pentadienoate (**14**) to 2-Oxo[3-D]pent-4-enoate [3-D]**15** in D_2O and Conversion to [3-D]Malate (**13**).* The stereochemical analysis of [3-D]**15**, generated in D_2O by the action of either wild type MIF or the K32A mutant on **14**, was performed by the modification of a literature procedure (*22*). Accordingly, each reaction mixture consisted of enzyme (MIF, 34 μg; and K32A, 900 μg) and **14** (4 mg) dissolved in DMSO-d_6 (30 μL). Individual reactions (18 for MIF and 22 for K32A) were carried out in 100 mM Na_2DPO_4 (0.6 mL, pD 9.1 in D_2O). The addition of **14** lowered the pD to ~6.8. The individual reaction mixtures were allowed to run at room temperature for either 2.5 (MIF) or 3.25 min (K32A). Reactions were quenched with 20 μL of a 300 mg/mL solution of $NaBH_4$ in 100 mM Na_2DPO_4 in D_2O after 2.5 (MIF) or 3.25 min (K32A) and pooled. The product, **16**, was isolated and converted to [3-D]malate (**12**) as described previously (*22*). The diastereomeric [3-D]-D,L-malate (MIF, 7 mg; and K32A, 8 mg) was purified by anion-exchange chromatography and treated with malic enzyme as described previously (*22*) to afford 2 mg of MIF or 2.5 mg of K32A of the (2*R*)-isomer of [3-D]malate (**13**, Scheme 5). (2*R*,3*S*)-[3-D]Malate (**13**) (from the MIF-catalyzed reaction): ^1H NMR (CD_3OD, 500 MHz) δ 2.62 (~0.9H, brd d, $J_{2,3}$ = 8.0 Hz, H3), 4.46 (~0.9H, brd d, $J_{2,3}$ = 8.0 Hz, H2). (2*R*,3*R*)-[3-D]Malate (from the MIF-catalyzed reaction): ^1H NMR (CD_3OD, 500 MHz) δ 2.76 (~0.1H, brd d, $J_{2,3}$ = 4.5 Hz, H3). (2*R*,3*S*)-[3-D]Malate (**13**) (from the K32A-catalyzed reaction): ^1H NMR (CD_3OD, 500 MHz) δ 2.62 (~0.6H, brd d, $J_{2,3}$ = 8.0 Hz, H3), 4.46 (~0.6H, brd d, $J_{2,3}$ = 8.0 Hz,

Scheme 5

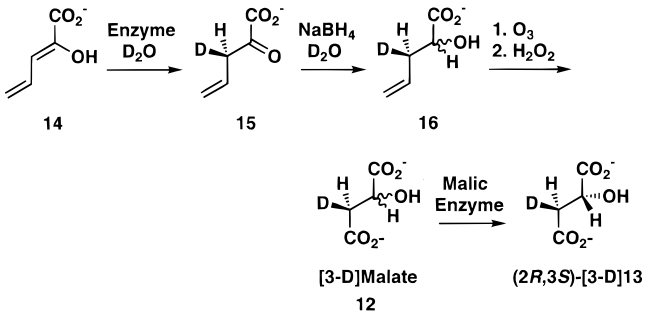

Table 1: Kinetic Parameters for the PPT Activity of MIF and the K32 Mutants[a]

enzyme	substrate	k_{cat} (s^{-1})	K_m (μM)	k_{cat}/K_m (M^{-1} s^{-1})	relative k_{cat}	relative k_{cat}/K_m
wild type	**3**	320 ± 80	150 ± 40	2.1×10^6	1.0	1.0
K32A	**3**	30 ± 10	180 ± 40	1.7×10^5	0.09	0.08
K32R	**3**	150 ± 10	100 ± 30	1.5×10^6	0.47	0.70
wild type	**5**	140 ± 20	200 ± 70	6.9×10^5	1.0	1.0
K32A	**5**	15 ± 2	140 ± 50	1.1×10^5	0.11	0.16
K32R	**5**	160 ± 30	350 ± 90	4.6×10^5	1.1	0.67

[a] The steady-state kinetics parameters were determined at 23 °C and pH 6.5. Errors are standard deviations.

H2). (2*R*,3*R*)-[3-D]Malate (from the K32A-catalyzed reaction): ^{1}H NMR (CD_3OD, 500 MHz) δ 2.76 (~0.4H, brd q, H3).

RESULTS

Production, Expression, and Characterization of the K32 Mutants. Two mutants of MIF (K32A and K32R) were constructed by overlap extension PCR, expressed in *E. coli* strain BL21(DE3)pLysS, and purified to >95% (as determined by SDS−PAGE) using a modification of a previously described procedure (*12*, *19*). The DNA sequence of each mutant was confirmed by DNA sequencing. The two mutants were also analyzed by ESI-MS and circular dichroism. The monomeric molecular masses determined for MIF and the K32 mutants are in excellent agreement with the predicted masses. The molecular masses also confirmed that the initiating *N*-formylmethionine had been removed. The CD spectra of the K32 mutants were comparable to that of the wild type MIF, indicating that the mutations did not result in any major conformational changes (data not shown).

Steady-State Kinetic Parameters of the K32 Mutants. The steady-state kinetic parameters for the PPT activity of the K32 mutants were measured using **3** and **5** as substrates, and compared to the parameters for the PPT activity of wild type MIF (Table 1). Two conclusions can be made on the basis of these data. First, the K_m values for the mutant-catalyzed reactions (using **3** and **5**) do not significantly differ from those obtained for the wild type. Second, only the K32A mutation has an effect on the k_{cat} and k_{cat}/K_m values. There is an 11-fold decrease in k_{cat} using **3** and a 9-fold decrease in k_{cat} using **5**. This results in a 12-fold decrease in k_{cat}/K_m for **3** and a 6-fold decrease in k_{cat}/K_m for **5**.

*pH Dependence of the Kinetic Parameters Using **3***. The pH dependence of k_{cat}/K_m and k_{cat} was measured for the PPT activity of MIF, K32A MIF, and K32R MIF using **3** (Figure 1A−C). For MIF and the K32R mutant, the pH−rate profile for k_{cat}/K_m versus pH exhibits a single ascending limb with a slope of 1 (panels A and B of Figure 1). A nonlinear least-squares fit of the pH dependence of k_{cat}/K_m to the logarithmic form of

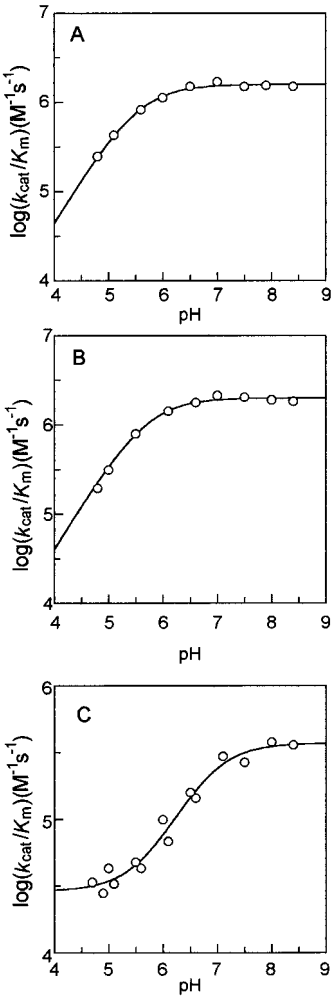

FIGURE 1: pH dependence of k_{cat}/K_m for the PPT activity of (A) MIF, (B) K32R MIF, and (C) K32A MIF using **3**. The curves were generated by a nonlinear least-squares fit of the data to eq 1. The pK_a values are given in the text.

$$k_{cat}/K_m = (k_{cat}/K_m)^{max}/(1 + [H^+]/K_{HE}) \quad (1)$$

where K_{HE} corresponds to the ionization constant for the free enzyme and $(k_{cat}/K_m)^{max}$ corresponds to the maximal value for this parameter gives the pK_a values (*11*, *22*, *26*). For the PPT activity of MIF, a pK_a value of 5.5 ± 0.1 is measured (Figure 1A). A pK_a of 6.0 ± 0.1 has previously been measured for the pH dependence of the k_{cat}/K_m using **4** (*11*). The slight difference in these pK_a values may result from the different assays used for their measurement. The higher pK_a value was measured using an indirect assay in that it monitors the formation of the borate complex of **3** generated by the enolization of **4** (*20*). The value reported here was measured using an assay that follows directly the ketonization of **3** to **4** (*12*), and is comparable to that measured by direct titration of Pro-1 by NMR spectroscopy (5.6 ± 0.1) (*10*). For the PPT activity of K32R MIF, a pK_a value of 5.7 ± 0.1 is measured (Figure 1B).

The plots of k_{cat} versus pH for these two proteins also exhibit a single ascending limb with a slope of 1 (data not shown). A nonlinear least-squares fit of the pH dependence

of k_{cat} to the logarithmic form of

$$k_{cat} = (k_{cat})^{max}/(1 + [H^+]/K_{HES}) \quad (2)$$

where K_{HES} corresponds to the ionization constant for the enzyme−substrate complex gives the pK_a values (*11*, *22*, *26*). For the PPT activity of both MIF and the K32R mutant, a pK_a value of 5.5 ± 0.2 is measured.

The pH dependence of k_{cat}/K_m and k_{cat} for the PPT activity of K32A MIF using **3** is more complex (Figure 1C). For the pH dependence of k_{cat}/K_m, a leveling off is seen at low pH such that protonation decreases the activity but does not result in the complete loss of activity. A statistically better fit of the data is obtained by a nonlinear least-squares fit of the pH dependence of k_{cat}/K_m to the logarithmic form of

$$k_{cat}/K_m = (k_{cat}/K_m)^{max}(1 + [H^+]/K_{H2E})/(1 + [H^+]/K_{HE}) \quad (3)$$

where K_{H2E} and K_{HE} correspond to two ionization constants for the free enzyme (*27*). This yields pK_a values of 5.7 ± 0.2 and 6.8 ± 0.1 for the free enzyme. The latter pK_a value is likely that of Pro-1.

The pH dependence of k_{cat} shows the same behavior as that observed for the pH dependence of k_{cat}/K_m (data not shown). Again, a statistically better fit of the data is obtained by a nonlinear least-squares fit of the pH dependence of k_{cat} to the logarithmic form of

$$k_{cat} = (k_{cat})^{max}(1 + [H^+]/K_{H2ES})/(1 + [H^+]/K_{HES}) \quad (4)$$

where K_{H2E} and K_{HES} correspond to two ionization constants for the enzyme−substrate complex (*27*). The pK_a values of 6.2 ± 0.3 and 7.2 ± 0.2 are measured.

*Competitive Inhibition Studies of the K32 Mutants with **7** and **10***. Both **7** and **10** have previously been reported to be competitive inhibitors of the PPT activity of MIF with K_i values of 2.6 ± 0.3 and 310 ± 60 μM, respectively (*11*, *12*, *14*). These compounds are also competitive inhibitors of the PPT activity of the K32A mutant with K_i values of 40 ± 4 and 375 ± 60 μM, respectively. Likewise, they are competitive inhibitors of the PPT activity of the K32R mutant having K_i values of 30 ± 3 and 234 ± 30 μM, respectively. The results show that replacing the lysine-32 with alanine causes a 15-fold decrease in the potency of **7** while replacing the lysine with arginine causes only an 11-fold decrease in potency. In contrast, these mutations have little effect on the potency of **10** as a competitive inhibitor. There is a 1.2-fold decrease in the potency for K32A and a 1.3-fold increase in the potency for K32R.

*Stereochemical Analysis of the MIF-, K32A-, and K32R-Catalyzed Reactions Using **3***. It has previously been shown that PPT catalyzes the stereospecific exchange of the *pro-R* proton of **4** (*28*). It was determined that (3*R*)-[3-D]**4** has a negative Cotton effect at 319 nm and a small positive effect at 252.5 nm (*28*). In this analysis, [3-D]**4** is generated in situ and a CD spectrum of the entire enzymatic reaction is recorded. Because the presence of the protein may preclude an accurate determination of the degree of stereoselectivity, particularly if the mutant-catalyzed reactions require much higher protein concentrations, an alternate protocol was devised (Scheme 4).

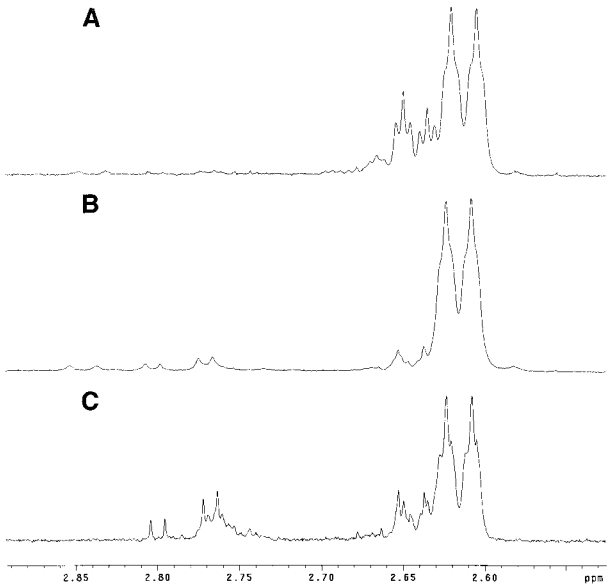

FIGURE 2: ^{1}H NMR (500 MHz, CD_3OD) spectrum of (2*R*)-[3-D]-malate obtained from the chemical and enzymatic conversion of [3-D]**4** generated by the PPT activity of (A) MIF, (B) K32A MIF, and (C) K32R MIF in D_2O. The other signals in the spectrum correspond to the fully protio malate and other impurities.

In this protocol, the stereochemical analysis of [3-D]**4** is carried out by its chemical and enzymatic conversion to (2*R*)-[3-D]malate (**13**) (Scheme 4). Accordingly, the addition of enzyme (MIF, K32A MIF, or K32R MIF) catalyzes the ketonization of **3** to [3-D]**4**, in D_2O. The immediate addition of $NaBH_4$ reduces [3-D]**4** to [3-D]**11** and prevents the epimerization of C-3. Degradation of [3-D]**11** to [3-D]**12** is achieved by subjecting it to ozonolysis and treating the resulting ozonide with hydrogen peroxide (*24*). Subsequently, the (2*R*)- and (2*S*)-isomers of **12** are obtained because the reduction of **4** with $NaBH_4$ was stereorandom. Incubation of this mixture with malic enzyme generates the (2*R*)-isomer of [3-D]**13** (*25*), which is subjected to ^{1}H NMR analysis.

It has been previously reported that each diastereotopic proton at C-3 of the fully protio malate appears as a doublet of doublets at 2.33 and 2.63 ppm in D_2O (*29*). (In CD_3OD, these signals are shifted downfield and appear at 2.62 and 2.78 ppm.) Stereospecific incorporation of a deuteron at C-3 results in the loss of one signal and the collapse of the remaining signal into a broadened doublet (*30*). The resonances for (2*R*)-[3-D]malate have been assigned by the reaction of maleic acid with maleate hydratase in D_2O (*29*). The product of the enzymatic reaction is (2*R*,3*R*)-[3-D]malate and the resulting ^{1}H NMR spectrum shows the loss of the upfield signal (2.33 ppm) and the presence of a downfield doublet (2.66 ppm).

For all three enzyme-catalyzed reactions, the ^{1}H NMR spectra (recorded in CD_3OD) of the (2*R*)-[3-D]malate (**13**) derived from the series of reactions shown in Scheme 4 show one pertinent signal, the broadened doublet at 2.61 ppm (Figure 2A−C). The presence of the upfield signal indicates that (2*R*,3*S*)-[3-D]malate is the predominant product isolated in all three reactions. For the MIF-catalyzed reaction (Figure 2A), this isomer is obtained exclusively (within the limits of detection), indicating that the reaction is stereospecific. For the K32A-catalyzed reaction (Figure 2B), the integral (not shown) for the signal at 2.61 ppm is ~20-fold greater

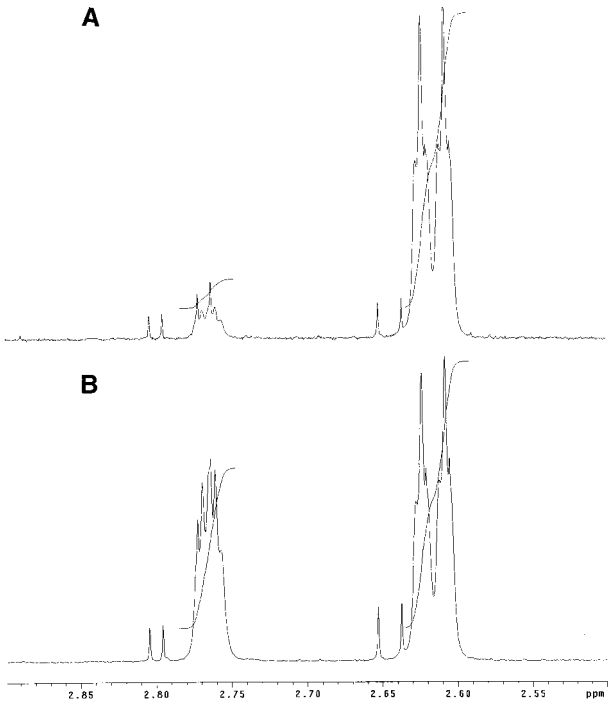

FIGURE 3: ^{1}H NMR (500 MHz, CD_3OD) spectrum of (2*R*)-[3-D]-malate obtained from the chemical and enzymatic conversion of [3-D]**15** generated by the PPT activity of (A) MIF and (B) K32A MIF in D_2O. The other signals in the spectrum correspond to the fully protio malate and other impurities.

than the integral corresponding to the signal at 2.76 ppm. Thus, the K32A-catalyzed reaction is highly stereoselective with the (2*R*,3*S*)-isomer predominating by a ratio of 20 to 1. For the K32R-catalyzed reaction (Figure 2C), the integral (not shown) for the signal at 2.61 ppm is only ~5-fold greater than the integral for the signal at 2.76 ppm. Thus, the K32R-catalyzed reaction is less stereoselective with the (2*R*,3*S*)-isomer predominating by only a ratio of 5 to 1.

The stereochemistry at C-3 of **13** indicates that the stereochemistry at C-3 of **11** is *R*. The priority numbering changes because a phenyl group replaces the carboxylate group at C-4. The stereochemistry at C-3 of **11** indicates that MIF catalyzes the ketonization of **3** to (3*R*)-[3-D]**4** (Scheme 4). This observation is in accord with the stereochemical results obtained previously (*28*).

*Stereochemical Analysis of the MIF- and K32A-Catalyzed Reactions Using 2-Hydroxy-2,4-pentadienoate (**14**).* The stereochemistry of the PPT activity of MIF and K32A MIF was also investigated using **14** (Scheme 5), a compound in which the phenyl ring has been replaced with a double bond. In preliminary studies,[2] it has been shown that MIF catalyzes the conversion of **14** to **15** (Scheme 5) with a K_m of 760 ± 110 μM, a k_{cat} of 160 ± 20 s^{-1}, and k_{cat}/K_m of 2.1×10^5 M^{-1} s^{-1}.

In D_2O, MIF or the K32A mutant converts **14** to [3-D]**15** (Scheme 5). Reduction of [3-D]**15** with $NaBH_4$ generates [3-D]**16**. The subsequent stereochemical analysis of [3-D]-**16** was based on its further chemical and enzymatic conversion to (2*R*,3*S*)-[3-D]malate (**13**) as described above and elsewhere (*22*, *25*). The ^{1}H NMR spectrum (Figure 3A) of the (2*R*)-[3-D]malate derived from [3-D]**15** in the MIF-catalyzed reaction exhibits two signals for the diastereotopic protons at C-3, one at 2.62 ppm and the other at 2.76 ppm, and indicates that a mixture of the (3*S*)- (2.62 ppm) and (3*R*)-isomers (2.76 ppm) has been obtained. The height of the integral for the signal at 2.62 ppm is ~10-fold greater than that of the signal at 2.76 ppm. Thus, the MIF-catalyzed conversion of **14** to **15** is highly stereoselective with the (2*R*,3*S*)-isomer predominating by a ratio of 10 to 1. For the K32A-catalyzed reaction, the ^{1}H NMR spectrum (Figure 3B) of the (2*R*)-[3-D]malate derived from [3-D]**15** exhibits the same two signals, indicating that a mixture of isomers has been obtained. However, the height of the signal at 2.62 ppm is now only ~2-fold greater than that of the signal at 2.76 ppm. Although the K32A-catalyzed reaction is stereoselective, the (2*R*,3*S*)-isomer now predominates only by a ratio of 2 to 1.

The stereochemistry at C-3 of **13** indicates that the stereochemistry at C-3 of **16** is *R*. The priority numbering changes because a double bond replaces the carboxylate group at C-4. The stereochemistry at C-3 of **16** indicates that MIF and the K32 mutant catalyze the ketonization of **14** to (3*R*)-[3-D]**15** (Scheme 5). As has been shown above and elsewhere (*28*), MIF catalyzes the ketonization of **3** to (3*R*)-[3-D]**4**. On the basis of these two observations, it can be reasonably inferred that **14** and **3** bind in the same orientation in the active site of MIF.

DISCUSSION

Lysine-32 is one of the few residues conserved in all 11 of the reported amino acid sequences of MIF and its homologues (*10*). This observation raises the question of whether Lys-32 plays a critical mechanistic or structural role either in the PPT activity of MIF or in one of its other biological activities. For the PPT activity of MIF, two roles for Lys-32 have been proposed primarily on the basis of crystallographic studies (*10*, *12*, *13*). Crystal structures of MIF, complexed with either **5** or **7**, clearly show an interaction between Lys-32 and the oxygen of the C-1 carboxylate group (*12*, *13*). In addition, these crystal structures and other studies suggest that the proximity of the positive charge of Lys-32 to Pro-1, the catalytic base, may be one of the factors responsible for lowering the pK_a of Pro-1 (*10*, *13*). In this study, the role of Lys-32 in the PPT activity was characterized by investigating the consequences of replacing it with a positively charged residue (arginine) and with an uncharged residue (alanine).

Mutation of Lys-32 to either alanine or arginine has surprisingly little effect on the kinetic parameters of the PPT activity even though a more substantial effect might have been anticipated on the basis of the observations made in the crystal structure (*12*, *13*). Using either **3** or **5**, the K_m values for both mutants are comparable to those determined for the wild type. If these K_m values reflect the substrate's binding affinity, then the results suggest that neither the loss of the electrostatic interaction with the carboxylate oxygen (K32A) nor the extra steric bulk of arginine (K32R) has a detrimental effect on substrate binding. Moreover, the extra steric bulk of arginine does not affect the reaction chemistry, product release, or both as there is little change in k_{cat} or k_{cat}/K_m. Replacement of lysine with an alanine does result in modest decreases in the values of k_{cat} and k_{cat}/K_m. Part of

[2] S. L. Stamps and C. P. Whitman, 1998, unpublished results.

the decrease in activity can be attributed to the fact that at pH 6.5 a significant fraction of the enzyme is not in the correct protonation state to act as a catalytic base (vide infra).

Our results also show that the PPT reaction of MIF is highly stereoselective (within the limits of detection) and that the high degree of stereoselectivity is only minimally perturbed when lysine is replaced with alanine and somewhat more adversely affected when the lysine is replaced with an arginine. On the basis of the two crystal structures (*12*, *13*) and the inhibition data obtained for compounds **7**−**10** (*14*), it can be inferred that **3** binds to MIF in the (*E*)-configuration and that the carboxylate group interacts with both Lys-32 and Ile-64. The high degree of stereoselectivity observed in the PPT reaction of K32A MIF would suggest that the electrostatic interaction between the lysine and the carboxylate oxygen is not a key stereochemical determinant. In addition to Lys-32 and Ile-64, interactions between the phenyl group of **3** and several residues of MIF which form a hydrophobic cavity further favor the binding of the (*E*)-isomer (*12*, *13*). Evidently, these interactions hold the substrate firmly in place and maintain access to only one face, the *re* face of **3**. The more significant decrease in the stereoselectivity of the K32R mutant has two plausible explanations. The first explanation is due to the fact that arginine is not sterically comparable to lysine and may take up more space in the active site. The additional bulk may skew the substrate in such a way that Pro-1 can now protonate the *si* face of **3**. Alternatively, arginine may be involved in a bidentate interaction with the carboxylate group, which may similarly skew the substrate. Nonetheless, the (3*R*)-isomer of [3-D]**4** is the predominant product, which would indicate that these effects are not major ones.

These kinetic and stereochemical results have one further implication. They confirm that the structural integrity of the active sites of these mutants is largely intact as both mutants process substrate with kinetic and stereochemical parameters similar to those of the wild type. Thus, it can be inferred from this observation and the fact that the CD spectra of the two mutants are comparable to that of the wild type that Lys-32 is not a critical structural residue.

To assess the contribution of the interaction between the phenyl group and the hydrophobic binding pocket to the stereochemical fidelity of the PPT-catalyzed reaction, the stereoselectivity of the MIF- and K32A-catalyzed reaction was determined using **14**. Replacement of the phenyl group with the smaller double bond should decrease the strength of the interaction between **14** and the active site of the protein. This would presumably allow for greater flexibility and thereby decrease the stereoselectivity of the reaction. The stereochemical studies support this hypothesis and suggest three additional conclusions. First, the ketonization of **14** by either the wild type or the K32A mutant generates predominantly the (3*R*)-isomer of [3-D]**15**. Likewise, MIF and K32A convert **3** to the (3*R*)-isomer of [3-D]**4**. These observations indicate that **3** and **14** bind comparably in the active site such that Lys-32 binds one carboxylate group while the side chain of Ile-64 binds the other carboxylate group. Second, the binding of the phenyl group of the substrate is more important for the stereochemical fidelity of the reaction than is the electrostatic interaction between Lys-32 and the carboxylate oxygen. This conclusion is based on the observation that the ketonization of **14** by the wild type protein is significantly less stereoselective than the K32A-catalyzed ketonization of **3**. Finally, the loss of both interactions (binding of the phenyl group and the electrostatic interaction) severely compromises the stereochemical integrity of the reaction as indicated by the very low stereoselectivity of the K32A-catalyzed ketonization of **14**. The remaining interaction between the carboxylate oxygen of **14** and the amide group of Ile-64 may be responsible for the residual stereoselectivity.

A more subtle effect of these mutations on the active site topology is revealed by competitive inhibition studies using **7** and **10**. Our results show that the inhibitory potency of **7** is affected more significantly than that of **10**. This observation is consistent with the differential inhibition data reported for a series of chemically stable enol analogues in addition to **7**−**10** that inhibit PPT (*14*). The binding potency of these compounds has been correlated with various structural features. One critical feature is the stereochemistry. The more potent inhibitors are those in which the phenyl group and the carboxylate group are on the same side of the double bond [(*E*)-**7** and (*Z*)-**9**]. A crystal structure of MIF·**7** shows that the carboxylate oxygens interact with Pro-1 and Lys-32 while the phenyl group interacts with the same residues described above for the binding of substrate (*12*, *13*). Thus, replacing the lysine with an alanine will decrease the affinity of **7** for the protein but not **10**, while replacing the lysine with an arginine is more likely to interfere with the binding of **7** and not that of **10**. Moreover, even though these mutations do affect the K_i values for **7** more significantly, these values are still ∼8−10-fold lower than the K_i values measured for **10**. The difference provides a rough approximation of the contribution made to binding by the interaction between **7** and Pro-1.

The most dramatic effect of the mutation of Lys-32 is seen in the pH dependence of the K32A- and K32R-catalyzed reactions. Removing the positive charge of lysine-32 increases the pK_a of the catalytic base by 1.3 units, and replacing the positive charge of lysine-32 with another positive charge returns the pK_a of the catalytic base to that of the wild type. The increase in the pK_a for Pro-1 in the K32A mutant partially accounts for the observed decreases in k_{cat} and k_{cat}/K_m because these parameters were measured at pH 6.5 where ∼67% of enzyme is in the wrong protonation state. At this pH, the catalytic base is in the charged state in which it is not able to act as a general base. Correcting the observed value of k_{cat}/K_m (1.7×10^5 M^{-1} s^{-1}) by the fraction of K32A in the correct protonation state yields a second-order rate constant of 5.1×10^5 M^{-1} s^{-1}, which is only 4-fold lower than the observed k_{cat}/K_m value for wild type activity.

These results provide additional evidence that the low pK_a value observed for the catalytic proline of MIF is due in part to the proximity of a positively charged residue, either lysine or arginine. Crystallographic studies have shown that Pro-1 is located at the bottom of a hydrophobic pocket (*10*, *12*, *13*). Two cationic groups, lysine-32 and lysine-66, are located nearby (*10*, *13*). Placing Pro-1 in this environment favors the neutral form, thereby lowering the pK_a. Removal of one of these features, a nearby positively charged residue, increases the pK_a. These observations contrast with the conclusions of a study on the structural basis of the low pK_a in 4-oxalocrotonate tautomerase (4-OT), a bacterial isomerase with which MIF is structurally homologous (*31*−*33*). For

4-OT, it has been determined that the hydrophobic pocket is primarily responsible for lowering the pK_a value and that the electrostatic effects of two nearby arginines (Arg-11 and Arg-39) have little influence (*22*).

MIF, 4-OT, and another bacterial isomerase, 5-(carboxymethyl)-2-hydroxymuconate isomerase (CHMI), are classified as members of an enzyme superfamily because they are structurally homologous and share several mechanistic features, most notably the catalytic amino-terminal proline (*31*). Two of our results have implications for the further delineation of the characteristics of this superfamily. The first observation, discussed above, is that MIF and 4-OT employ different mechanisms to lower the pK_a of the catalytic proline. The second observation is that MIF, like 4-OT, converts **14** to (3*R*)-[3-D]**15**, although the MIF-catalyzed reaction is more stereoselective. For MIF, the (3*R*)-isomer predominates by a ratio of ~10 to 1, while for 4-OT, the (3*R*)-isomer predominates only by a ratio of ~1.7 to 1 (*22*, *34*). The fact that the same isomer is generated implies that **14** is bound similarly at the active sites of the two proteins and that Pro-1 occupies the same position relative to the bound substrate. This reinforces the supposition that the members of this superfamily are related by their ability to catalyze the keto−enol tautomerization of a pyruvyl moiety (*11*). The difference in the stereoselectivity of the two reactions is presumably a reflection of the different specificity of the two proteins. MIF prefers a phenyl group attached to a pyruvyl or enolpyruvyl moiety (e.g., **3**−**6**), while 4-OT prefers a carboxylate group attached to C-5 of **14** (*22*). Because of this difference, **14** may be more firmly fixed within the active site of MIF than it is within the active site of 4-OT. Finally, while it is clear that MIF functions as a tautomerase and interconverts **14** and **15**, it is not yet certain whether MIF will generate the α,β-isomer from **14** (or a related dienol) as does 4-OT (*22*, *34*). Addressing this question will be of considerable interest in defining further the reactions catalyzed by MIF and the characteristics of the superfamily (*11*).

CONCLUSIONS

Lysine-32, an active site residue in the PPT activity of MIF, was mutated to alanine and arginine, and several kinetic and stereochemical parameters were determined and compared to those of the wild type. Major effects on the kinetic parameters and the stereochemical fidelity of the K32A- and K32R-catalyzed reactions were not found. However, a 1.3 unit increase in the pK_a of Pro-1 was measured for the K32A mutant. Together, these observations indicate that the primary function of Lys-32 in the PPT activity of MIF is to lower the pK_a of the catalytic base. The stereoselectivity of the MIF- and K32A-catalyzed reactions using 2-hydroxy-2,4-pentadienoate was also determined. The results define the roles of different active site interactions in maintaining the stereochemical fidelity of the reaction.

ACKNOWLEDGMENT

We are grateful to Dr. R. Bucala for providing us with the clone containing the recombinant mouse MIF. We thank Steve D. Sorey (Department of Chemistry, The University of Texas) for his expert assistance in the acquisition of the ^{1}H NMR spectra on the Varian Unity INOVA-500 spectrometer. Electrospray ionization mass spectrometry was performed by the analytical instrumentation service core supported by Center Grant ES 07784.

REFERENCES

1. Bloom, B. R., and Bennett, B. (1966) *Science 153*, 80−82.
2. Bernhagen, J., Mitchell, R. A., Calandra, T., Voelter, W., Cerami, A., and Bucala, R. (1994) *Biochemistry 33*, 14144−14155.
3. Calandra, T., Bernhagen, J., Metz, C. N., Spiegel, L. A., Bacher, M., Donnelly, T., Cerami, A., and Bucala, R. (1995) *Nature 377*, 68−71.
4. Bucala, R. (1996) *FASEB J. 10*, 1607−1613.
5. Bernhagen, J., Calandra, T., Mitchell, R. A., Martin, S. B., Tracey, K. J., Voelter, W., Manogue, K. R., Cerami, A., and Bucala, R. (1993) *Nature 365*, 756−759.
6. Donnelly, S. C., Haslett, C., Reid, P. T., Grant, I. A., Wallace, W. A. H., Metz, C. N., Bruce, L. J., and Bucala, R. (1997) *Nat. Med. 3*, 320−323.
7. Rice, G. C., Liittschwager, K., Metz, C., and Bucala, R. (1998) *Annu. Rep. Med. Chem. 33*, 243−252.
8. Rosengren, E., Aman, P., Thelin, S., Hansson, C., Ahlfors, S., Bjork, P., Jacobsson, L., and Rorsman, H. (1997) *FEBS Lett. 417*, 85−88.
9. Bendrat, K., Al-Abed, Y., Callaway, D. J. E., Peng, T., Calandra, T., Metz, C. N., and Bucala, R. (1997) *Biochemistry 36*, 15356−15362.
10. Swope, M., Sun, H.-W., Blake, P., and Lolis, E. (1998) *EMBO J. 17*, 3534−3541.
11. Stamps, S. L., Fitzgerald, M. C., and Whitman, C. P. (1998) *Biochemistry 37*, 10195−10202.
12. Taylor, A. B., Johnson, W. H., Jr., Czerwinski, R. M., Li, H.-S., Hackert, M. L., and Whitman, C. P. (1999) *Biochemistry 38*, 7444−7452.
13. Lubetsky, J. B., Swope, M., Dealwis, C., Blake, P., and Lolis, E. (1999) *Biochemistry 38*, 7346−7354.
14. Pirrung, M. C., Chen, J., Rowley, E. G., and McPhail, A. T. (1993) *J. Am. Chem. Soc. 115*, 7103−7110.
15. Sambrook, J., Fritsch, E. F., and Maniatis, T. (1989) *Molecular Cloning: A Laboratory Manual*, Cold Spring Harbor Laboratory Press, Cold Spring Harbor, NY.
16. Stanley, T. M., Johnson, W. H., Jr., Burks, E. A., Whitman, C. P., Hwang, C.-C., and Cook, P. F. (1999) *Biochemistry* (submitted for publication).
17. Laemmli, U. K. (1970) *Nature 227*, 680−685.
18. Ho, S. N., Hunt, H. D., Horton, R. M., Pullen, J. K., and Pease, L. R. (1989) *Gene 77*, 51−59.
19. Czerwinski, R. M., Johnson, W. H., Jr., Whitman, C. P., Harris, T. K., Abeygunawardana, C., and Mildvan, A. S. (1997) *Biochemistry 36*, 14551−14560.
20. Knox, W. E., and Pitt, B. M. (1957) *J. Biol. Chem. 225*, 675−688.
21. Larsen, P. O., and Wieczorkowska, E. (1974) *Acta Chem. Scand. B 28*, 92−96.
22. Harris, T. K., Czerwinski, R. M., Johnson, W. H., Jr., Legler, P. M., Harris, T. K., Abeygunawardana, C., Massiah, M. A., Stivers, J. T., Whitman, C. P., and Mildvan, A. S. (1999) *Biochemistry 38*, 12343−12357.
23. Pouchert, C. J., and Behnke, J. (1993) *The Aldrich Library of ^{13}C and ^{1}H FT NMR Spectra*, Vol. 2, p 1024C, Aldrich Chemical Co., Milwaukee, WI.
24. Arakawa, H. (1963) *Naturwissenschaften 50*, 441.
25. Spina, J., Bright, H. J., and Rosenbloom, J. (1970) *Biochemistry 9*, 3794−3800.
26. Stivers, J. T., Abeygunawardana, C., Mildvan, A. S., Hajipour, G., and Whitman, C. P. (1996) *Biochemistry 35*, 814−823.
27. Cleland, W. W. (1977) *Adv. Enzymol. 45*, 273−387.
28. Retey, J., Bartl, K., Ripp, E., and Hull, W. E. (1977) *Eur. J. Biochem. 72*, 251−257.

29. Gawron, O., Glaid, A. J., and Fondy, T. P. (1961) *J. Am. Chem. Soc. 83*, 3634−3640.
30. Englard, S., Britten, J. S., and Listowsky, I. (1967) *J. Biol. Chem. 242*, 2255−2259.
31. Murzin, A. G. (1996) *Curr. Opin. Struct. Biol. 6*, 386−394.
32. Stivers, J. T., Abeygunawardana, C., Mildvan, A. S., Hajipour, G., Whitman, C. P., and Chen, L. H. (1996) *Biochemistry 35*, 803−813.
33. Taylor, A. B., Czerwinski, R. M., Johnson, W. H., Jr., Whitman, C. P., and Hackert, M. L. (1998) *Biochemistry 37*, 14692−14700.
34. Lian, H., and Whitman, C. P. (1993) *J. Am. Chem. Soc. 115*, 7978−7984.

BI991825S